Journal of Alloys and Compounds 509 (2011) 942–947

Contents lists available at ScienceDirect

Journal of Alloys and Compounds

journal homepage: www.elsevier.com/locate/jallcom

Properties of praseodymium-doped bismuth potassium titanate ($Bi_{0.5}K_{0.5}TiO_3$) synthesised using the soft combustion technique

Chai Yan Ng, Khairunisak Abdul Razak*

School of Materials and Mineral Resources Engineering, Universiti Sains Malaysia, 14300 Nibong Tebal, Penang, Malaysia

ARTICLE INFO

Article history:
Received 19 July 2010
Received in revised form
22 September 2010
Accepted 23 September 2010
Available online 1 October 2010

Keywords:
Ceramics
Chemical synthesis
Dielectric response
Microstructure

ABSTRACT

Bismuth potassium titanate ($Bi_{0.5}K_{0.5}TiO_3$; BKT) and praseodymium-doped BKT ($Bi_{0.5(1-x)}Pr_xK_{0.5}TiO_3$; BPKT) powders were synthesised using the soft combustion technique. Fine particles of 10–100 nm of BKT and BPKT were produced. A single phase BKT was obtained with a minimum of 0.5 mol of glycine. Various compounds of $Bi_{0.5(1-x)}Pr_xK_{0.5}TiO_3$ where $x = 0.01$, 0.03, 0.05, 0.10, 0.15 and 0.20 were prepared. Pure BKT and BPKT powders were obtained after calcination at 800 °C for 3 h. After sintering at 1050 °C for 5 h, pure BKT and BPKT pellets were obtained for $x = 0$ and 0.01. However, for BPKT with $x = 0.03$, 0.05, 0.10, 0.15 and 0.20, a minor amount of $Bi_4Ti_3O_{12}$ (BIT) secondary phase was present after sintering at 1050 °C for 5 h. The crystallite size and grain size of all the samples followed similar trends, first increasing from $x = 0$ (undoped BKT) to $x = 0.05$ and then decreasing above $x = 0.05$. Among the undoped and doped samples, BPKT with $x = 0.05$ had the highest dielectric properties ($\varepsilon_r = 713.87$) due to its large crystallite size (68.66 nm), large grain size (~435 nm) and high relative density (93.39%).

1. Introduction

Lead-based piezoelectric materials are known for their hazards to health and negative environmental impact. Moreover, because lead is volatile above 800 °C and thus can be more hazardous as it is released into the environment, researchers are actively seeking to replace lead with lead-free materials. Potassium sodium niobates ($K_{0.5}Na_{0.5}NbO_3$; KNN) and bismuth sodium titanate ($Bi_{0.5}Na_{0.5}TiO_3$; BNT) are among the most studied lead-free piezoelectric materials [1]. In addition, bismuth potassium titanate ($Bi_{0.5}K_{0.5}TiO_3$; BKT), a well-known Bi-based perovskite piezoelectric ceramic, is also one of the candidates for lead-free piezoelectrics due to its excellent electrical properties and high Curie temperature (T_c) of 380 °C. However, only a few studies on BKT ceramics have been reported. This lack of information may be due to the difficulty of producing a high density BKT ceramic because Bi and K are volatile at high sintering temperatures [2,3].

BKT powders have been prepared typically by common methods of solid state reaction [2,4,5], sol–gel technique [6,7] and hydrothermal technique [8]. The solid state reaction method has the advantages of ease of implementation and its ability to synthesise compounds in large amounts. However, the powders usually tend to agglomerate and have inhomogeneous particle size [6,9,10]. The sol–gel technique has excellent compositional control and homogeneity on the molecular level, yet the derived precipitates are amorphous in nature [6]. On the other hand, the hydrothermal technique is capable of yielding high-purity, fine crystalline powders [8]. Nevertheless, this synthesis in an aqueous environment causes water to be incorporated into the powder, thus causing deterioration in the electrical properties [11]. The soft combustion technique can produce fine particle size powder from the nanometre to the submicron scale and requires a low sintering temperature (1050 °C). Sintering at this lower temperature can minimise the volatilisation of Bi and K ions. Furthermore, this soft combustion technique requires only simple equipment, has a low cost and allows better control of stoichiometry [12]. Hence, the current work used the soft combustion technique to prepare the samples.

Furthermore, to improve the electrical properties of BKT, praseodymium (Pr) was doped in BKT to produce $Bi_{0.5(1-x)}Pr_xK_{0.5}TiO_3$ (BPKT). Pr is a lanthanide element that has a tendency to reduce the Bi and O vacancies in the BKT. In addition, Pr^{3+} has a six-coordinated ionic radius (0.99 Å), which is close to the ionic radius of Bi^{3+} (1.03 Å), suggesting that Pr ions may easily replace the Bi ions with a small lattice distortion [13]. In this paper, the morphologies, structural and dielectric properties of the BKT and BPKT are reported.

2. Experimental details

The $Bi_{0.5}K_{0.5}TiO_3$ (with 0.1, 0.3, 0.5, 1.0 and 1.5 mol of glycine) and $Bi_{0.5-x}Pr_xK_{0.5}TiO_3$ (with $x = 0.01$, 0.03, 0.05, 0.10, 0.15 and 0.20) powders were synthesised using the soft combustion technique. For preparation of the BKT powder, bismuth (III) nitrate pentahydrate [$Bi(NO_3)_3{\cdot}5H_2O$], potassium nitrate (KNO_3) and titanium (IV) isopropoxide {$Ti[OCH(CH_3)_2]_4$} were used as the starting materials

* Corresponding author.
E-mail address: khairunisak@eng.usm.my (K.A. Razak).

0925-8388/$ – see front matter © 2010 Elsevier B.V. All rights reserved.
doi:10.1016/j.jallcom.2010.09.136

for Bi, K and Ti, respectively. First, KNO_3 and $Bi(NO_3)_3{\cdot}5H_2O$ were dissolved in 25 ml of 2-methoxyethanol ($CH_3OCH_2CH_2OH$) at 40 °C. However, KNO_3 could not be fully dissolved in the solution. Thus, KNO_3 was first dissolved in 5 ml of deionised water before mixing with $Bi(NO_3)_3{\cdot}5H_2O$. In addition, to aid in the combustion process, glycine (H_2NCH_2COOH), which acts as a combustion fuel, was added into $Bi(NO_3)_3{\cdot}5H_2O$. On the other hand, $Ti[OCH(CH_3)_2]_4$ was dissolved separately in 25 ml of $CH_3OCH_2CH_2OH$, with 5 ml of acetylacetone ($CH_3COCH_2COCH_3$) as the chelating agent to stabilise the mixture. Then the $Ti[OCH(CH_3)_2]_4$ solution was added to the Bi–K solution with continuous stirring, and the final mixture was stirred for 2 h.

Next, the mixture was heated to 130 °C on a hot plate with continuous stirring. Evaporation occurred, and a sticky gel was formed, followed by a soft combustion process (exothermic chemical reaction that resulted in the production of flame) that formed foam. This foam was then crushed in a mortar to obtain a fine powder. This synthesised powder was calcined at 800 °C for 3 h with a heating rate of 5 °C min^{-1} and a cooling rate of 10 °C min^{-1}. After calcination, the powder was pressed at a pressure of 55 bar into pellets 12 mm in diameter. Finally, the pellets were sintered at 1050 °C for 5 h at a heating rate of 5 °C min^{-1} and a cooling rate of 10 °C min^{-1} in a closed alumina crucible. For the preparation of BPKT powder, praseodymium (III) nitrate hexahydrate [$Pr(NO_3)_3{\cdot}6H_2O$] was dissolved together with the $Bi(NO_3)_3{\cdot}5H_2O$ and H_2NCH_2COOH in the beginning, and the remaining steps were similar to those for the preparation of the BKT.

The powders and sintered pellets were analysed for the presence of phases using an X-ray diffractometer (Bruker AXS D8 ADVANCE) equipped with Cu Kα radiation from 20° to 70°. The morphology of powders and sintered pellets was observed using a field emission scanning electron microscope (Zeiss SUPRA 35) and transmission electron microscope (Philips CM 12). Crystallite size was measured using Rietveld refinement, and the density of sintered pellets was measured using the Archimedes method. The dielectric properties of the pellets were measured using a LCR meter (Agilent HP4284) at 1 MHz and 1 V. Prior to dielectric measurement, silver paste was applied on both surfaces of the pellets for ohmic contact.

3. Results and discussion

First, the BKT powder was produced without dissolving KNO_3 in deionised water. Fig. 1(a) shows the XRD pattern of the powder after calcination at 800 °C. This XRD spectrum shows the presence of a secondary phase in the compounds, indicating that the process did not form a single phase BKT. The BKT phase matched the ICDD number of 36-0339, whereas the secondary phase matched the ICDD number (72-1019) of bismuth titanate ($Bi_4Ti_3O_{12}$; BIT). It could have been that KNO_3 had not been fully dissolved in the solution, causing the formation of the secondary phase, so thereafter, KNO_3 was first dissolved in 5 ml of deionised water.

The XRD spectrum of the calcined powder is shown in Fig. 1(b). Like the powder that had not been dissolved in deionised water, the BKT dissolved in 5 ml of deionised water also contained the secondary phase of BIT. However, the BIT peaks were not obvious in the spectrum. The most obvious peak was (1 1 7). It could be that the low intensity XRD peak reflects the presence of only a very small amount of the BIT phase. Thereafter, to minimise the presence of the secondary phase, all subsequent powders were produced by

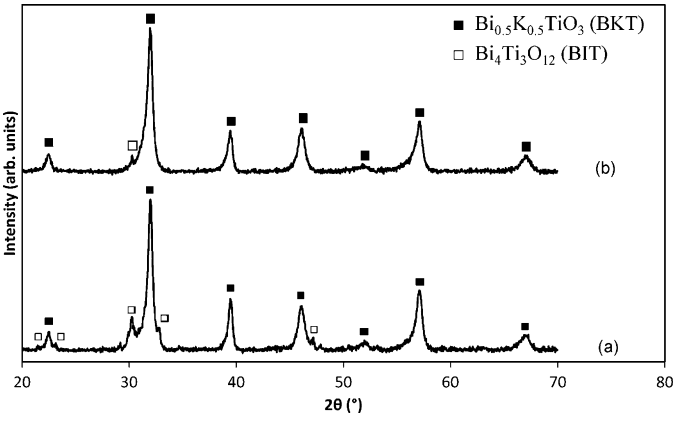

Fig. 1. XRD spectra of the BKT powders: (a) without dissolution in deionised water and (b) dissolved in 5 ml deionised water calcined at 800 °C.

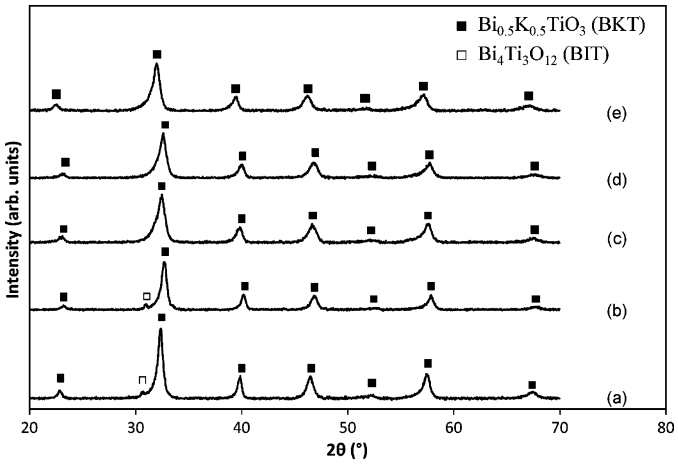

Fig. 2. XRD spectra of the BKT powders with: (a) 0.1 mol, (b) 0.3 mol, (c) 0.5 mol, (d) 1.0 mol and (e) 1.5 mol of glycine. All samples were calcined at 800 °C.

dissolving KNO_3 in 5 ml of deionised water during the preparation of BKT.

At this point, the calcined powder containing only a single phase BKT had not been obtained yet. It was thought that the presence of the secondary phase that remained even after dissolving KNO_3 in water could be due to incomplete combustion of the starting materials. Therefore, glycine (H_2NCH_2COOH) was added into the starting materials. Glycine is one of the most popular and attractive fuels for producing uniform composition and precisely controlled stoichiometry of complex oxide ceramic powders [14]. From the XRD spectra of BKT produced using various molar fractions of glycine (Fig. 2), it can be observed that the BKT synthesised with the addition of 0.1 and 0.3 mol of glycine, like the BKT synthesised without glycine, showed the presence of the secondary BIT phase. However, the BKT with 0.5, 1.0 and 1.5 mol of glycine showed the presence of only single phase BKT. The result indicates that the addition of a small amount of glycine (0.1 and 0.3 mol) was insufficient to enhance the combustion process, whereas a higher amount of glycine (0.5 mol and above) was sufficient to yield pure phase BKT. Thereafter, 0.5 mol of glycine was used to prepare the subsequent powders.

Fig. 3 shows the thermogravimetric analysis (TGA) curve of BKT powder with 0.5 mol of glycine. Weight losses were observed at 100–120 °C, 320–380 °C, 380–550 °C and 550–700 °C. Because water vaporises in the lowest temperature range, weight loss in this range was likely due to the loss of moisture from the sample. At 320–380 °C, the weight loss was likely due to the decomposition of organic substances. A gradual weight loss also occurred in the temperature range of 380–550 °C, also attributable

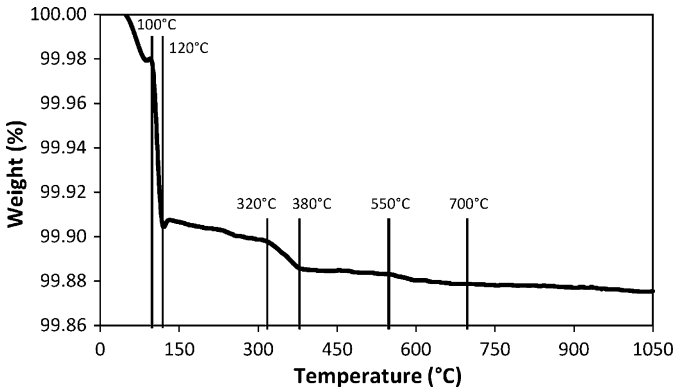

Fig. 3. TGA curve of the BKT powder with 0.5 mol of glycine.

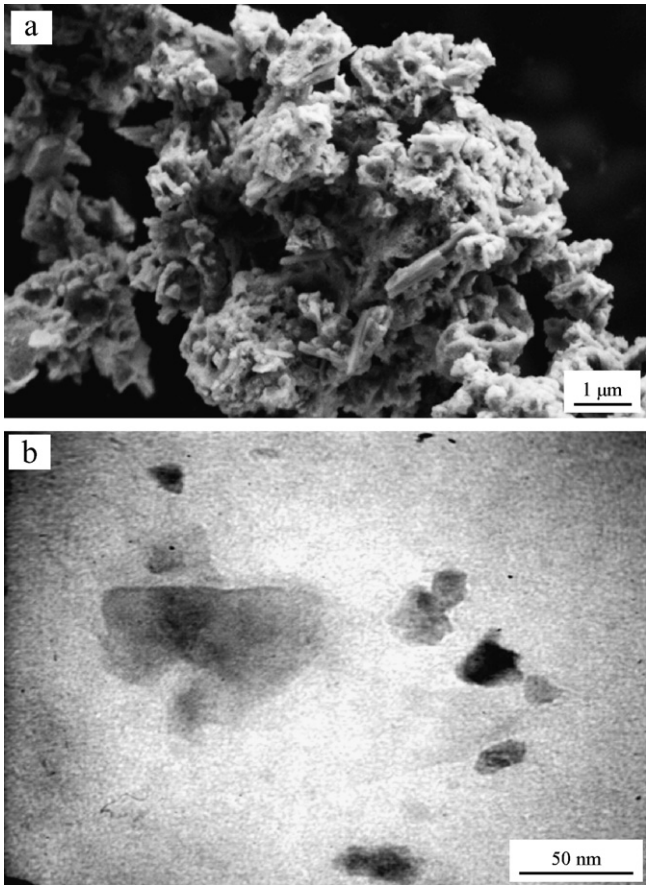

Fig. 4. (a) FESEM and (b) TEM micrographs of the calcined BKT powders produced using 0.5 mol of glycine.

to decomposition of physically and chemically absorbed water. Moreover, the decomposition of nitrate materials of $Bi(NO_3)_3{\cdot}5H_2O$ and KNO_3 also took place at this temperature [15]. In addition, weight loss was also observed at 550–700 °C. This weight loss could be due to the solid state reaction of the starting materials to

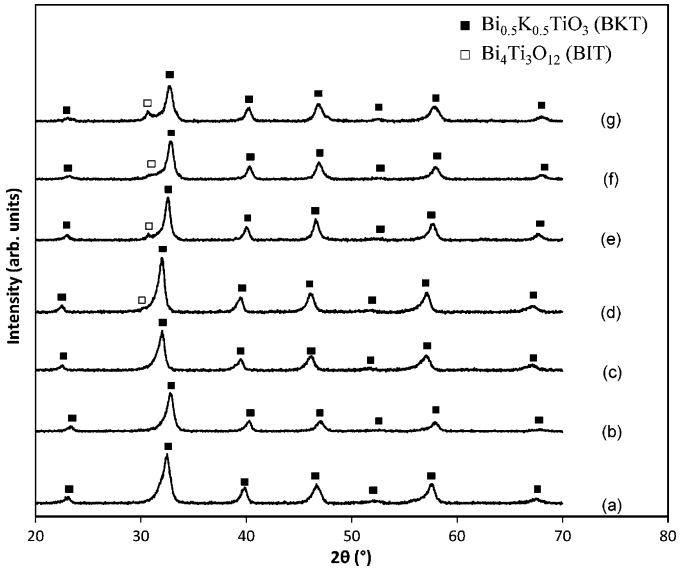

Fig. 5. XRD spectra of the BPKT powders with varying x calcined at 800 °C: (a) 0 (BKT), (b) 0.01, (c) 0.03, (d) 0.05, (e) 0.10, (f) 0.15 and (g) 0.20.

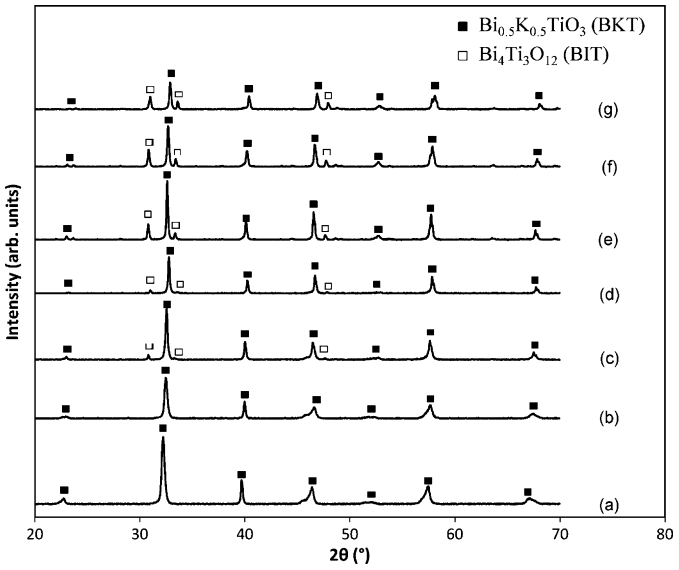

Fig. 6. XRD spectra of the BPKT pellets with varying x sintered at 1050 °C: (a) 0, (b) 0.01, (c) 0.03, (d) 0.05, (e) 0.10, (f) 0.15 and (g) 0.20.

form BKT powder. Above 700 °C, there was no measurable weight change of the powder. This finding implies that complete reaction occurred at this temperature and formed BKT [15,16]. Hence, in this research the calcination temperature of BKT powder was set above 700 °C. The FESEM and TEM micrographs of the BKT powders (with 0.5 mol of glycine) after calcination at 800 °C are shown in Fig. 4. The BKT powders have flake-like particles in the range of 10–100 nm.

In this study, various amounts of Pr (x = 0.01, 0.03, 0.05, 0.10, 0.15, 0.20) were added to BKT to obtain $Bi_{0.5-x}Pr_xK_{0.5}TiO_3$ (BPKT). Fig. 5 shows the XRD spectra of the undoped BKT and various BPKT powders calcined at 800 °C. The BPKT with x = 0.01 and 0.03 show only single phase BPKT, indicating that the Pr^{3+} in the BPKT did not form a secondary phase or separate from the interior grain but instead dissolved into the perovskite lattice [17]. However, as the x increased (x = 0.05, 0.10, 0.15, 0.20), the secondary phase of BIT appeared. For the BPKT (x = 0.01) and BPKT (x = 0.03), the amount of Pr added was lower, and thus the secondary phase of BIT was not formed, whereas for the BPKT with x = 0.05, 0.10, 0.15 and 0.20, a small amount of the secondary phase was formed. The formation of the secondary BIT phase was due to the high level of Pr doping. When Pr was added to BKT, the Pr^{3+} substituted the Bi^{3+}, and these bondless Bi^{3+} ions then reacted with Ti^{4+} and O^{2-} to form

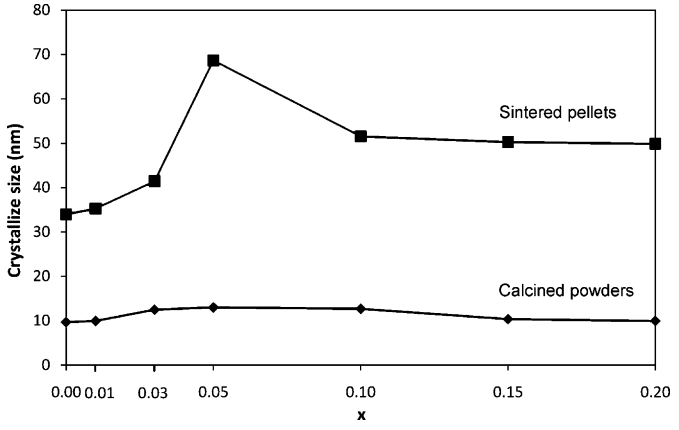

Fig. 7. Crystallite size of the calcined powders and sintered pellets of BKT and BPKT.

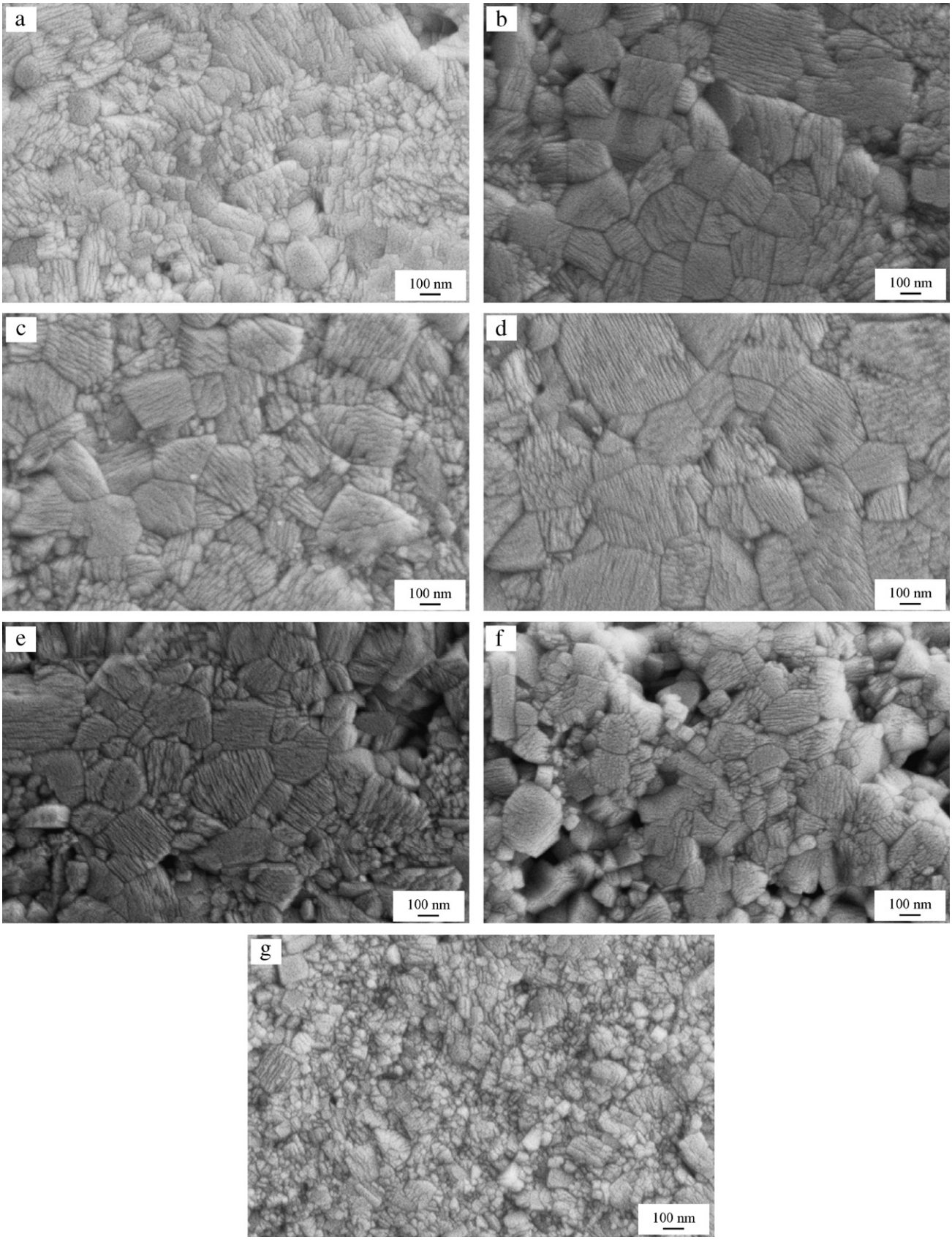

Fig. 8. FESEM micrographs of the BPKT with varying *x*: (a) 0, (b) 0.01, (c) 0.03, (d) 0.05, (e) 0.10, (f) 0.15 and (g) 0.20.

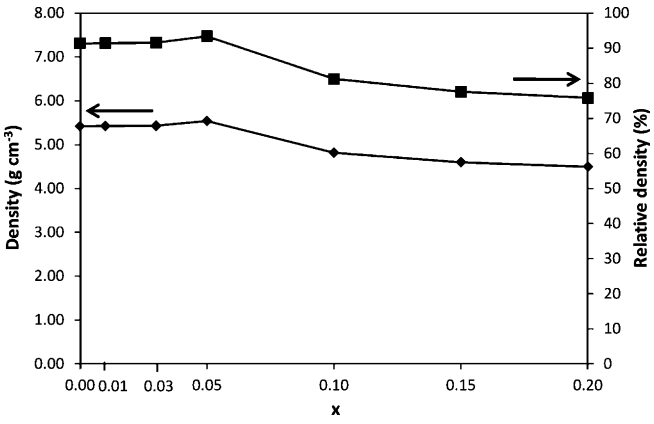

Fig. 9. Density and relative density of the sintered pellets.

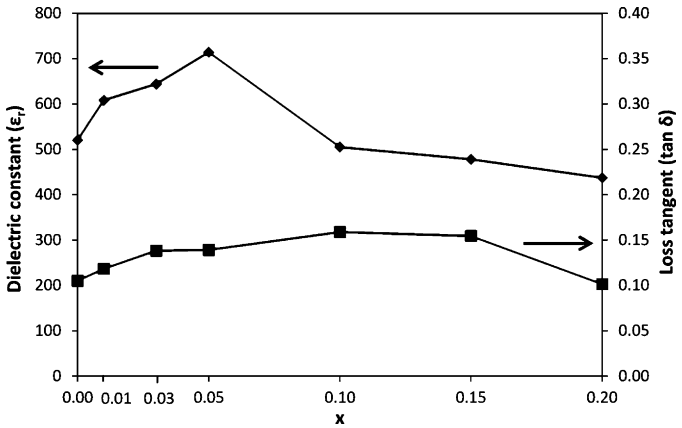

Fig. 10. Dielectric properties of BPKT with varying *x*.

BIT. The formation of the secondary BIT phase is not typical in BKT formation. Previous studies found the formation of BKT contained secondary phases of $Bi_2Ti_2O_7$ [18], $K_4Ti_3O_8$ [4], $K_2Ti_4O_9$ [2] and $K_2Ti_6O_{13}$ [2]. The presence of the BIT secondary phase could be explained by the volatilisation of K^+ and Bi^{3+} during the sintering process.

These calcined powders were then pressed into pellets and sintered at 1050 °C for 5 h. Fig. 6 shows the XRD spectra of the sintered BKT and BPKT pellets. These XRD spectra show that only the BKT and BPKT ($x = 0.01$) contained pure phase BKT and BPKT with no evidence of the presence of the secondary phase. For the BPKT pellets with $x = 0.03$, 0.05, 0.10, 0.15 and 0.20, the secondary phase of BIT was present. As the amount of Pr dopant increased, the intensities of the peaks for the BIT phase became stronger, indicating that the secondary BIT phase became more dominant (with higher crystallinity) as the amount of dopant increased. As the amount of Pr dopant increased, more Pr^{3+} were substituted for the Bi^{3+}; thus, more bondless Bi^{3+} were available to react with Ti^{4+} and O^{2-}, resulting in the formation of more BIT. Moreover, K also evaporates at the sintering temperature used. Hence, lower levels of K can lead to the formation of a more stable BIT.

The crystallite size of the calcined powders and sintered pellets was in the range of 9.66–13.01 nm and 33.98–68.66 nm, respectively. The plots of the crystallite size of calcined powders and sintered pellets against the amount of Pr (x) are shown in Fig. 7. It can be observed that the crystallite size of both calcined powders and sintered pellets increased from $x = 0$ to $x = 0.05$ and then decreased from $x = 0.05$ to $x = 0.20$. Because the BKT was doped with small amounts of Pr ($x = 0.01$–0.05), the Pr ions diffused into the BKT and assisted the growth of the grains. However, when the amount of Pr increased to $x = 0.10$, an obvious secondary BIT phase was formed. It is believed that this BIT phase acted as a grain growth inhibitor, thus suppressing the crystallite growth of the BPKT phase [12,19,20]. In addition, it can be seen that the crystallite size in the sintered pellets was larger than that in the calcined powders, probably because ion diffusion during the sintering process caused crystallite growth.

The FESEM micrographs of the sintered BKT and BPKT pellets are presented in Fig. 8. The grains showed no particular shape. The grain sizes of the BPKT increased when $x = 0$ (100–300 nm) to $x = 0.05$ and decreased between $x = 0.05$ and $x = 0.20$. The BPKT with $x = 0.05$ had the largest grain sizes, averaging 435 nm. This trend toward changing grain sizes aligns with the trend toward changing crystallite size that was observed in XRD analysis. This similarity is expected because crystallite size normally increases as grain size increases [12,21].

Fig. 9 shows the plots of density and relative density of the sintered pellets against x. The densities of the pellets increased from $x = 0$ to $x = 0.05$ and then decreased from $x = 0.05$ to $x = 0.20$. It could be that the addition of Pr caused the formation of close-packed microstructures with increasing grain size. The decrease in density was likely due to the decreasing grain size from $x = 0.05$. In addition, the decreasing density could be caused by the presence of more secondary phase.

The dielectric constant (ε_r) and loss tangent ($\tan\delta$) of the sintered pellets were found to be in the range of 437.19–713.87 and 0.1014–0.1589, respectively (Fig. 10). The ε_r increased up to $x = 0.05$ and decreased beyond $x = 0.05$. The undoped BKT had an ε_r of 520.1, while the BPKT ($x = 0.05$) had the highest ε_r of 713.87. This ε_r trend aligns with the trends of crystallite sizes and grain sizes, which is expected because the ε_r always increases with increasing grain sizes [5]. It is known that the electrical properties of ferroelectric ceramics are highly dependent on the grain size and microstructure of the samples [12]. As the ferroelectric ceramic was cooled through the T_c, stress appeared in the system. These stresses within the grains can be released or reduced by the formation of an appropriate arrangement of 90° domains. For larger grains, most of the stresses can be relieved with this mechanism. On the other hand, as the grain size decreases, the domains also become smaller. This domain width is roughly proportional to the square root of the grain size. The number of domains in a grain decreases as the square root of the grain size, and thus the smaller the grain, the larger the unrelieved stress [21–23]. Furthermore, the decrease of ε_r between $x = 0.05$ and $x = 0.20$ could also be due to the poor density. It is well known that low density ceramics have low ε_r as well. The values of $\tan\delta$ increased from $x = 0$ to $x = 0.10$ and then decreased from $x = 0.10$ to $x = 0.20$. The BPKT ($x = 0.05$) had the highest ε_r and an acceptable $\tan\delta$ of 0.1391, indicating that this BPKT can be used as a capacitor and in ferroelectric and piezoelectric devices.

4. Conclusions

BKT and BPKT were successfully produced using the soft combustion technique. The optimum amount of glycine added to aid the combustion reaction was found to be 0.5 M. Pure BPKT was obtained up to $x = 0.01$. Above that level, the ferroelectric compound BIT was formed. BPKT with $x = 0.05$ showed the optimum dielectric properties with a dielectric constant of 713.87 and $\tan\delta$ of 0.1391. The result was in agreement with the largest crystallite size and grain size, and the highest density was observed for BPKT with $x = 0.05$.

Acknowledgements

The authors express their sincere appreciation to the technical support of the School of Materials and Mineral Resources Engineering, Universiti Sains Malaysia. This research was supported by Research University grant 1001/PBahan/811069.

References

[1] L. Chen, H. Fan, M. Zhang, C. Yang, X. Chen, J. Alloys Compd. 492 (2010) 313–319.
[2] J. Konig, M. Spreitzer, B. Jancar, D. Suvorov, Z. Samardzija, A. Popovic, J. Eur. Ceram. Soc. 29 (2009) 1695–1701.
[3] T. Wada, A. Fukui, Y. Matsuo, Jpn. J. Appl. Phys. 41 (2002) 7025–7028.
[4] P.V.B. Rao, E.V. Ramana, T.B. Sankaram, J. Alloys Compd. 467 (2009) 293–298.
[5] Y. Hiruma, H. Nagata, T. Takenaka, Jpn. J. Appl. Phys. 46 (2007) 1081–1084.
[6] Y.D. Hou, L. Hou, S.Y. Huang, M.K. Zhu, H. Wang, H. Yan, Solid State Commun. 137 (2006) 658–661.
[7] X. Huang, Z. Yang, L. Sun, Q. Xie, B. Li, J. Zhou, L. Li, Mater. Chem. Phys. 114 (2009) 23–25.
[8] M.M. Lencka, M. Oledzka, R.E. Riman, Chem. Mater. 12 (2000) 1323–1330.
[9] X. Chen, Y. Liao, H. Wang, L. Mao, D. Xiao, J. Zhu, Q. Chen, J. Alloys Compd. 493 (2010) 368–371.
[10] H. Zhang, S. Jiang, K. Kajiyoshi, J. Alloys Compd. 495 (2010) 173–180.
[11] J.G. Lisoni, F.J. Piera, M. Sanchez, C.F. Soto, V.M. Fuenzalida, Appl. Surf. Sci. 134 (1998) 225–228.
[12] P.Y. Goh, K.A. Razak, S. Sreekantan, J. Alloys Compd. 475 (2009) 758–761.
[13] S.S. Kim, W.J. Kim, Thin Solid Films 484 (2005) 303–309.
[14] S.T. Aruna, A.S. Mukasyan, Curr. Opin. Solid State Mater. Sci. 12 (2008) 44–50.
[15] J. Hao, X. Wang, R. Chen, L. Li, Mater. Chem. Phys. 90 (2005) 282–285.
[16] C.S. Chou, J.H. Chen, R.Y. Yang, S.W. Chou, Powder Technol. 202 (2010) 39–45.
[17] U. Chon, J.S. Shim, H.M. Jang, J. Appl. Phys. 93 (2003) 4769–4775.
[18] Y. Zhang, X. Zheng, T. Zhang, L. Gong, S. Dai, Y. Chen, Sens. Actuators B: Chem. 147 (2010) 180–184.
[19] S. Kuharuangrong, J. Mater. Sci. 36 (2001) 1727–1733.
[20] H. Zhang, S. Jiang, K. Kajiyoshi, J. Xiao, J. Am. Ceram. Soc. 93 (2010) 750–757.
[21] V. Buscaglia, M.T. Buscaglia, M. Viviani, L. Mitoseriu, P. Nanni, V. Trefiletti, P. Piaggio, I. Gregora, T. Ostapchuk, J. Pokorny, J. Petzelt, J. Eur. Ceram. Soc. 26 (2006) 2889–2898.
[22] A.J. Moulson, J.M. Herbert, Electroceramics: Materials, Properties, Applications, 2nd edition, John Wiley & Sons, 2003.
[23] Z. Zhao, V. Buscaglia, M. Viviani, M.T. Buscaglia, L. Mitoseriu, A. Testino, M. Nygren, M. Johnsson, P. Nanni, Phys. Rev. B 70 (2004) 024107-1–124107-8.